

**Pawel A. Penczek**

**The University of Texas – Houston Medical School,  
Department of Biochemistry.**



**THE UNIVERSITY *of* TEXAS**

**HEALTH SCIENCE CENTER AT HOUSTON**

**MEDICAL SCHOOL**

# 3D reconstruction of helical filaments

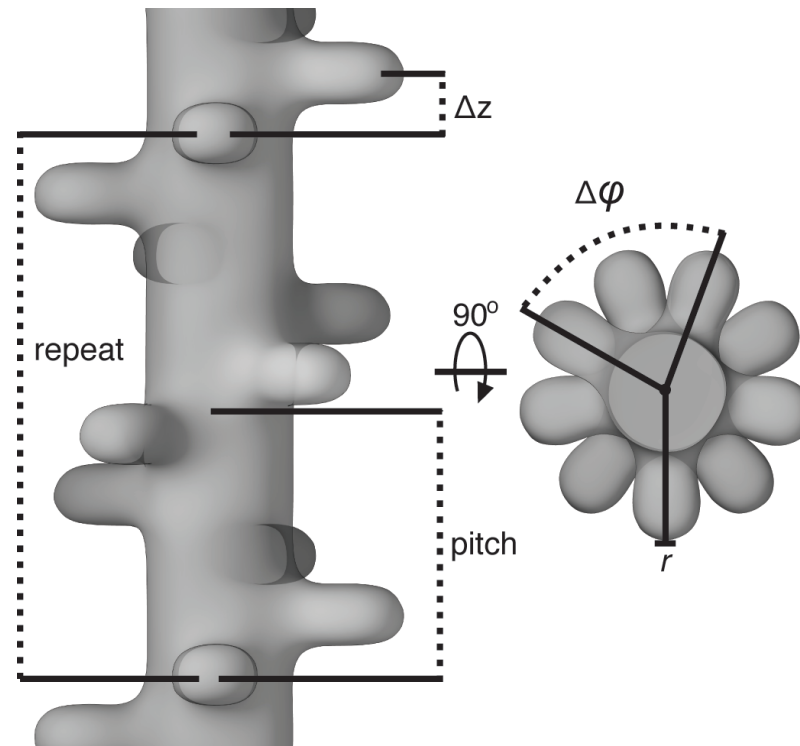
## helical symmetry:

azimuthal rotation per subunit  $\Delta\varphi$

axial subunit translation (rise)  $\Delta z$

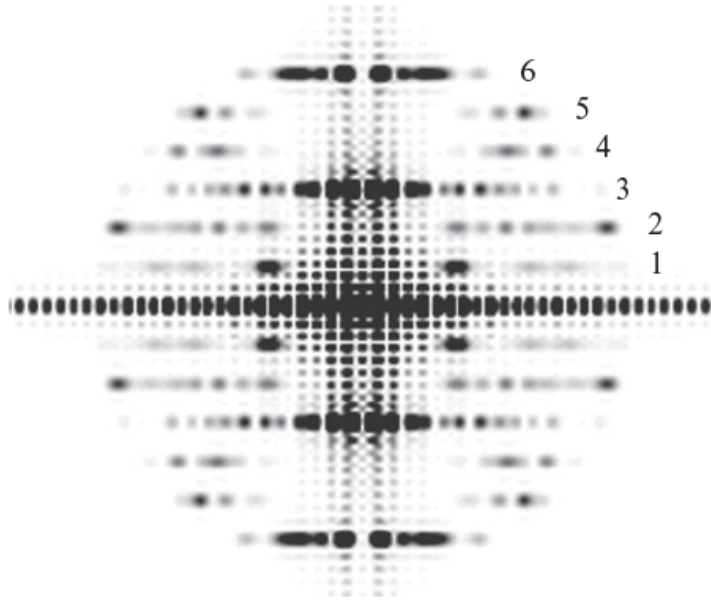
$$f(r, \varphi, z) = f(r, \varphi + n\Delta\varphi, z + n\Delta z), \quad n = \pm 1, \pm 2, \dots$$

$$r = \sqrt{x^2 + y^2}$$

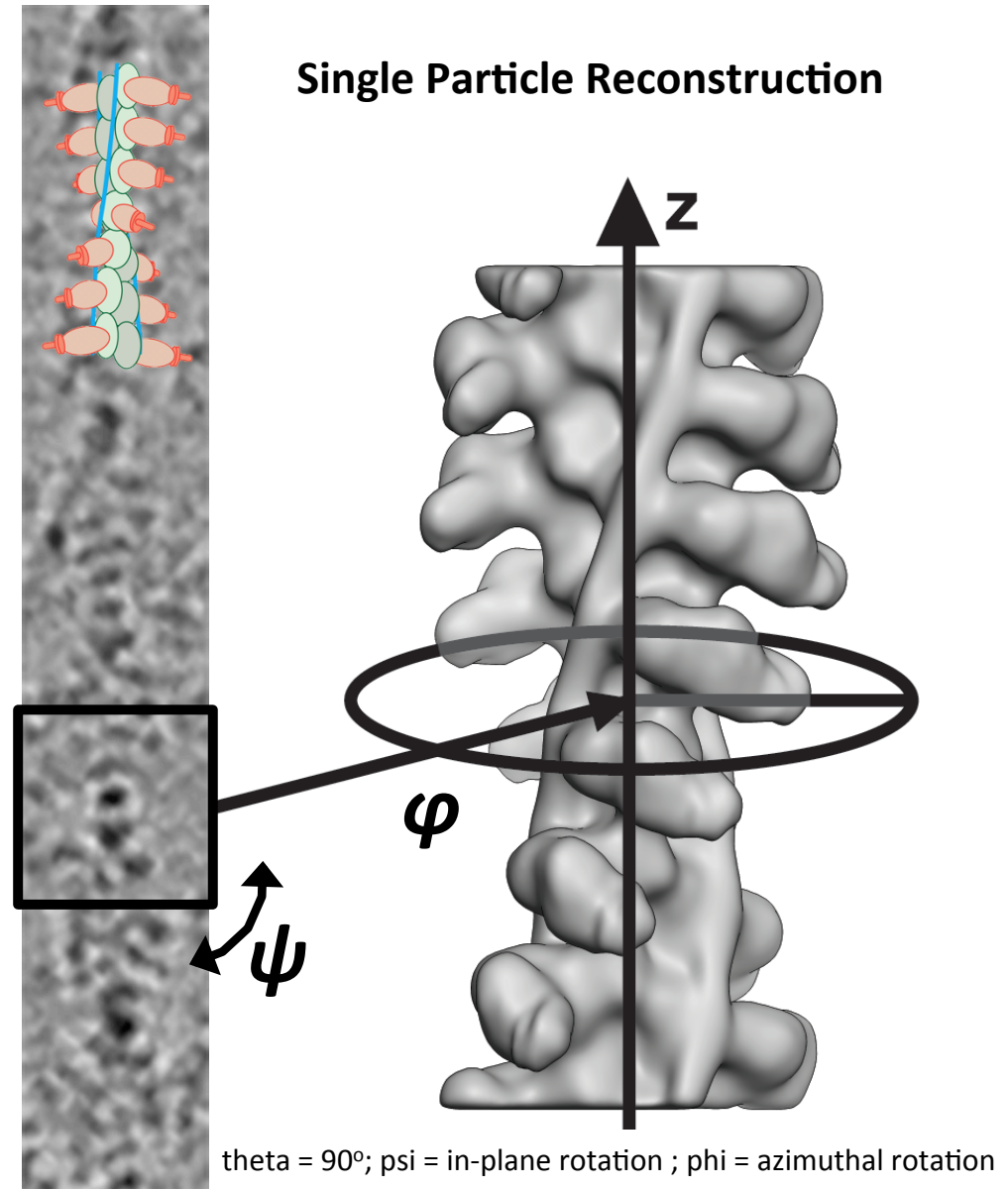


# Crystal or Single Particle with Symmetry?

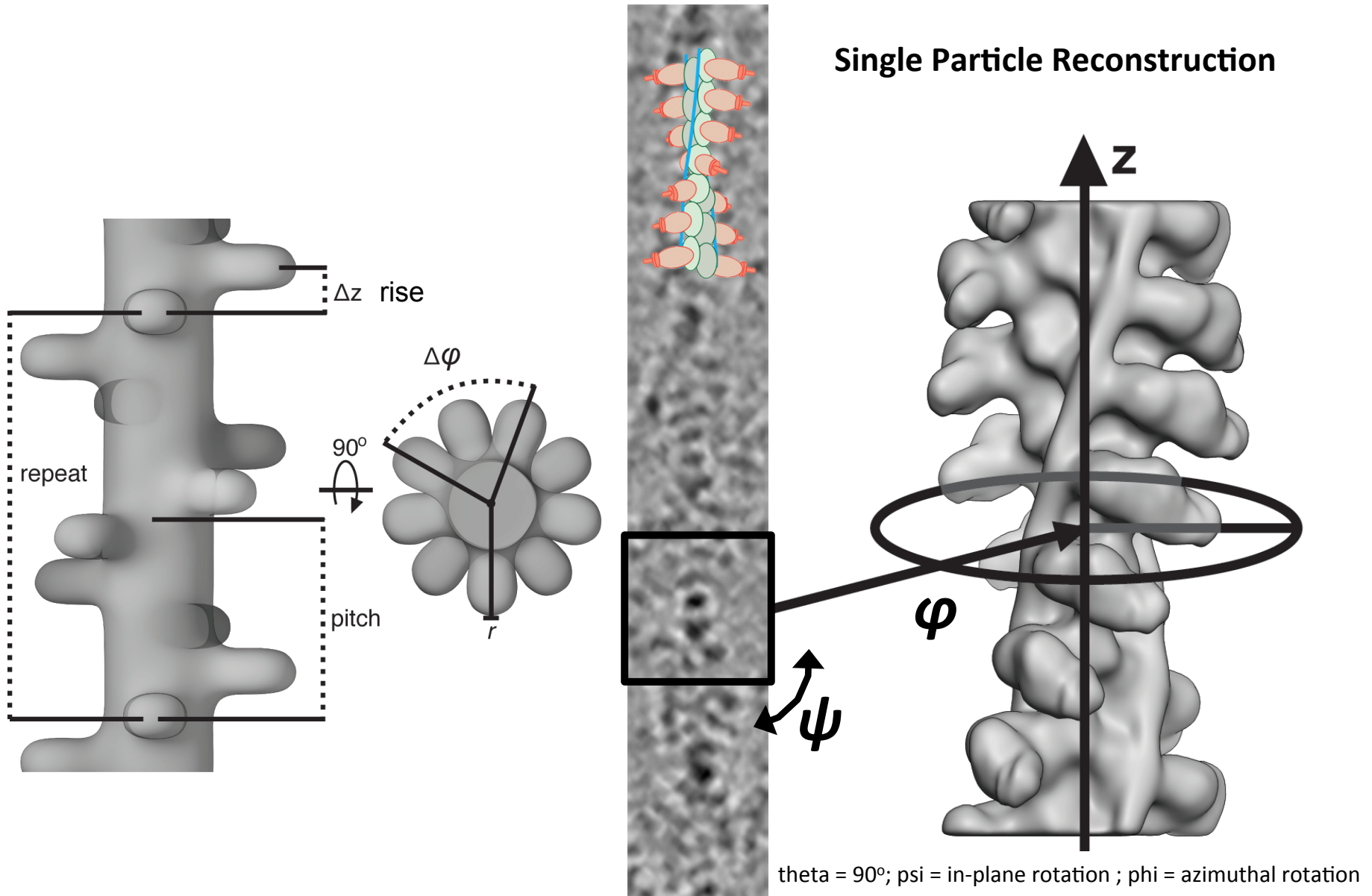
Fourier-Bessel Formalism



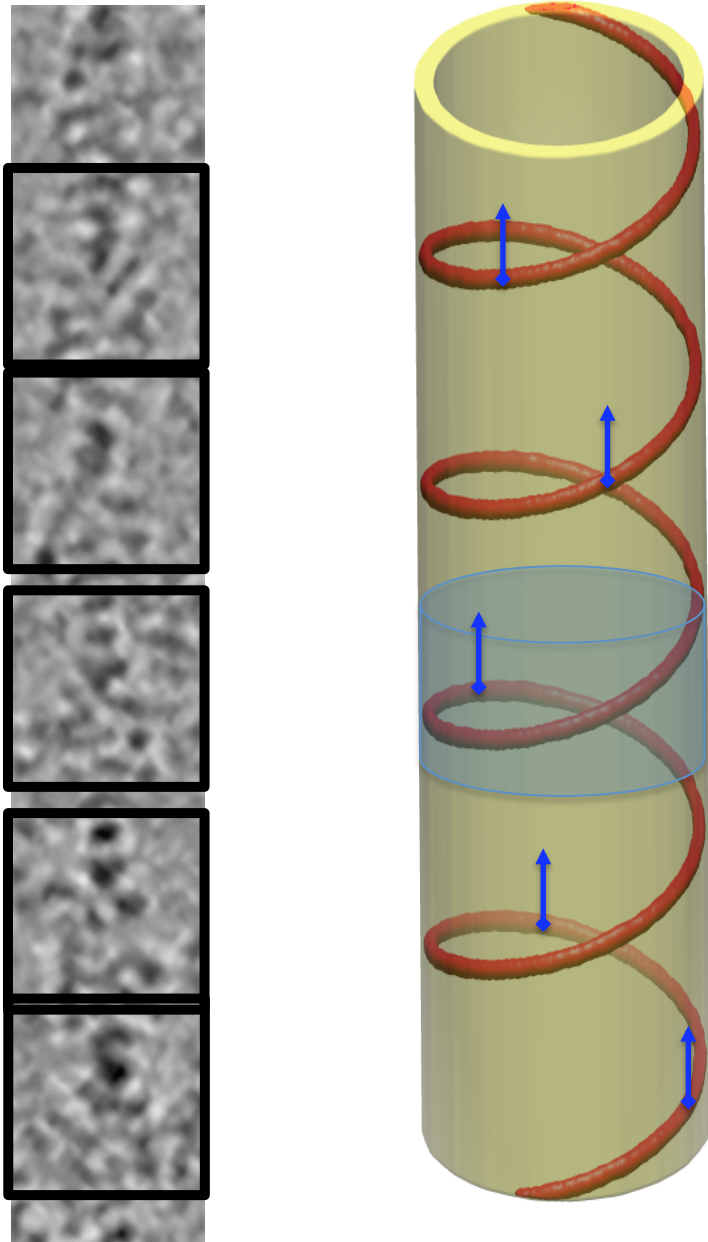
Single Particle Reconstruction



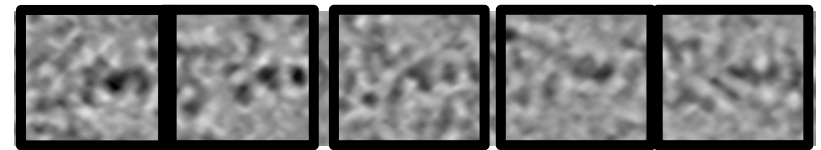
# Crystal or Single Particle with Symmetry?



# Single Particle Approach to Helical Filaments

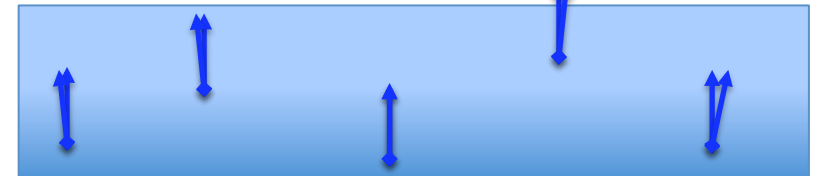


$$f(r, \varphi, z) = f(r, \varphi + n\Delta\varphi, z + n\Delta z), \quad n = \pm 1, \pm 2, \dots$$



rise

$\Delta z$



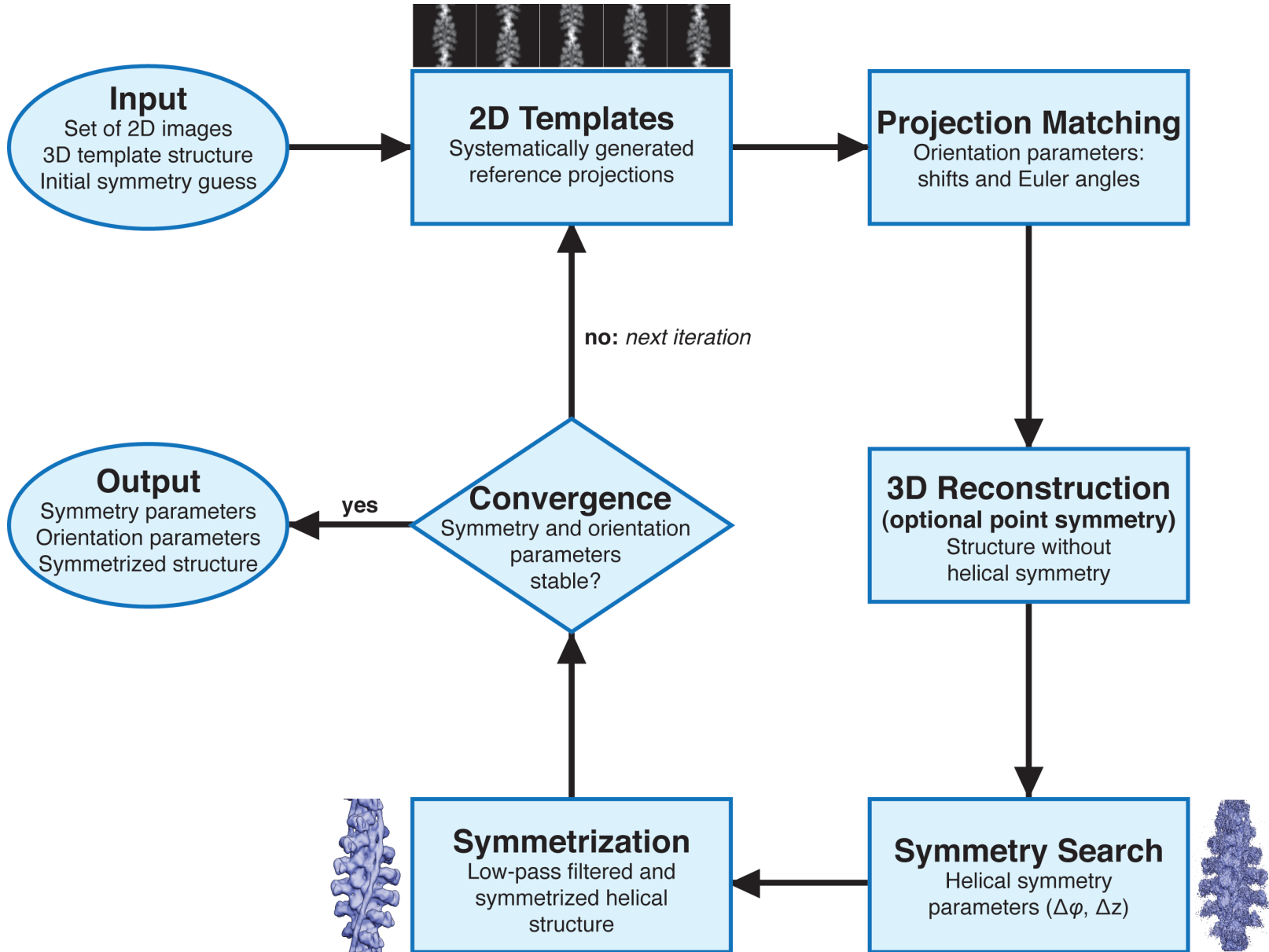
$0^\circ$

$\varphi$

$360^\circ$

If filaments were perfectly flat within the ice layer, all EM projection images would constitute orthoaxial projections of the filament and the problem would be to find three orientation parameters for each segment: angles  $\phi$  and  $\psi$  ( $\theta=90$ ) and translation along the main axis  $z$

# IHRSR



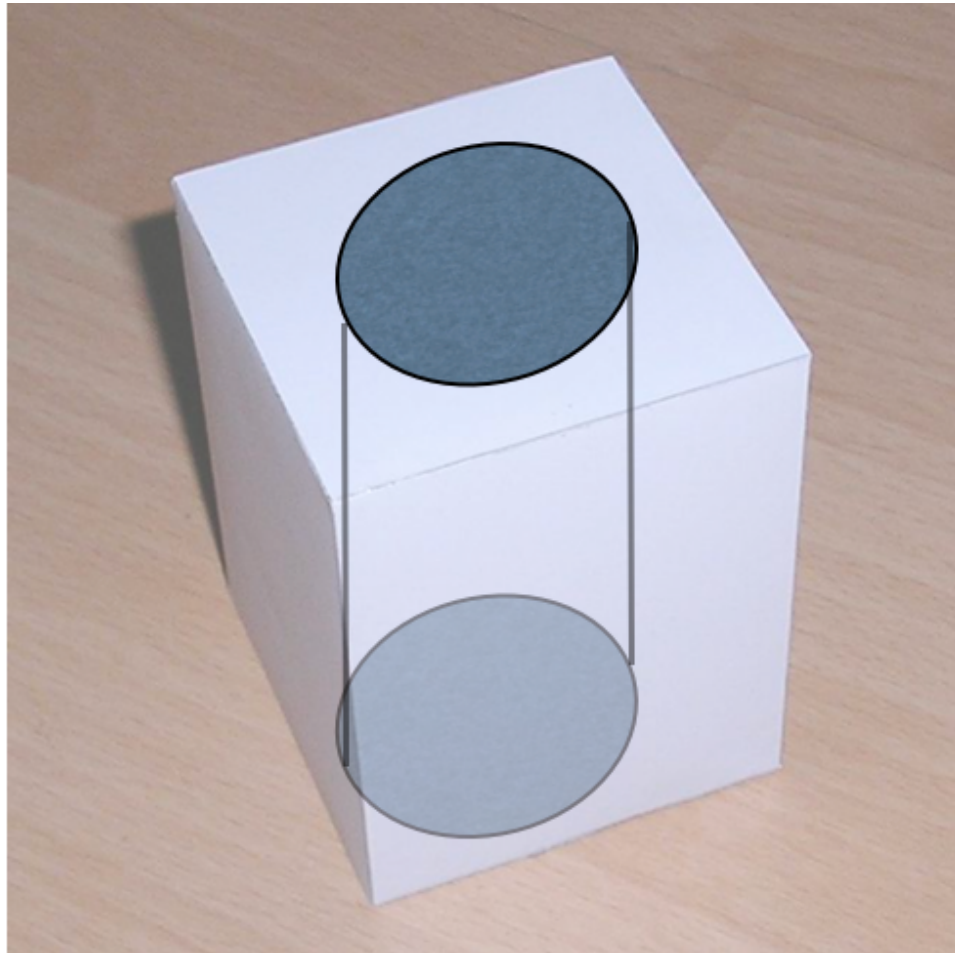
# IHRSR implementation in SPARX

1. new implementation offers more flexibility
2. orientation searches are done in a sensible way
3. point-group symmetries of helical filaments

## **New features:**

1. parallelization using python-level MPI makes it possible to execute the refinement rapidly on large clusters
2. restricted (constrained) search for in-plane rotation ( $\psi$ ) makes the procedure more robust (segments are pre-aligned along z-axis)
3. search for translation restricted to axial rise
4. search for helical symmetry implemented under MPI (it tends to be time consuming)
5. search for translation adapts itself to the current axial rise
6. out-of-plane tilt ( $\theta$  not equal 90) implemented!
7. 3D reconstruction and reprojections done within rectangular prism

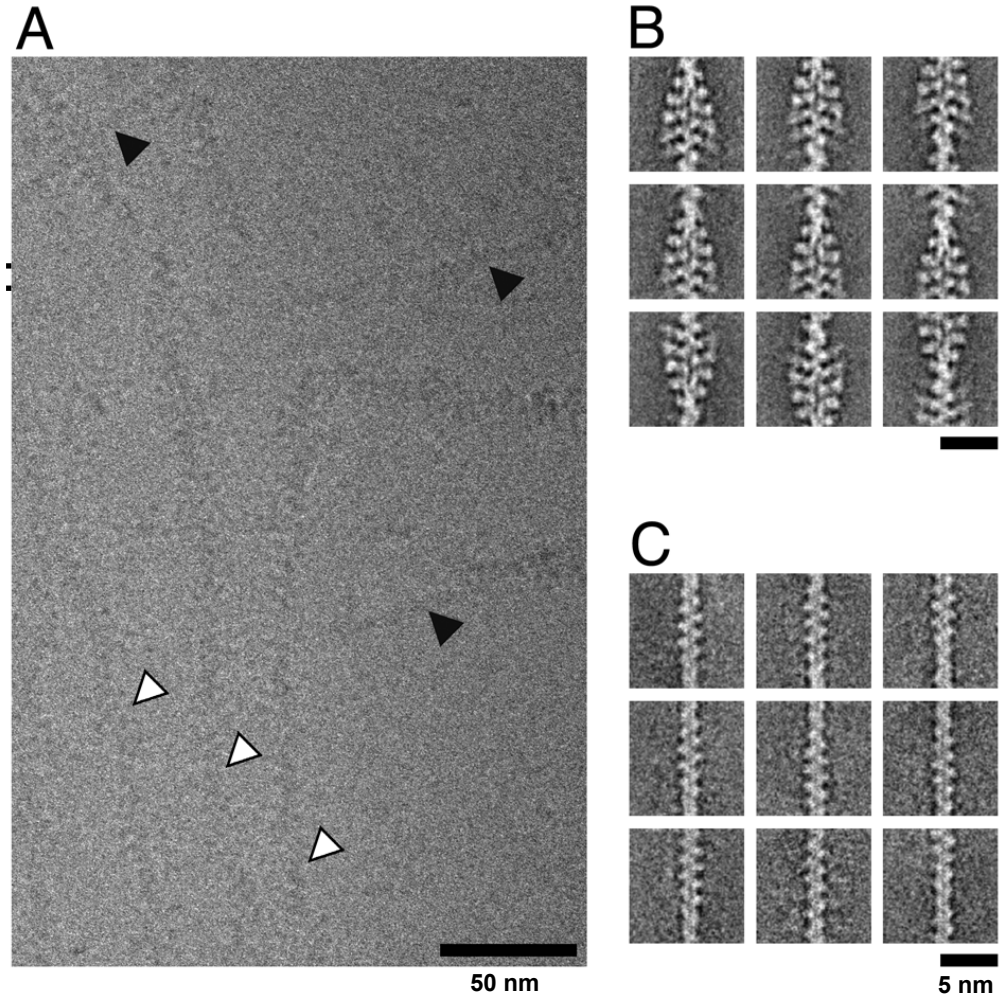
Rectangular prism geometry  
saves computer memory and time of calculations.



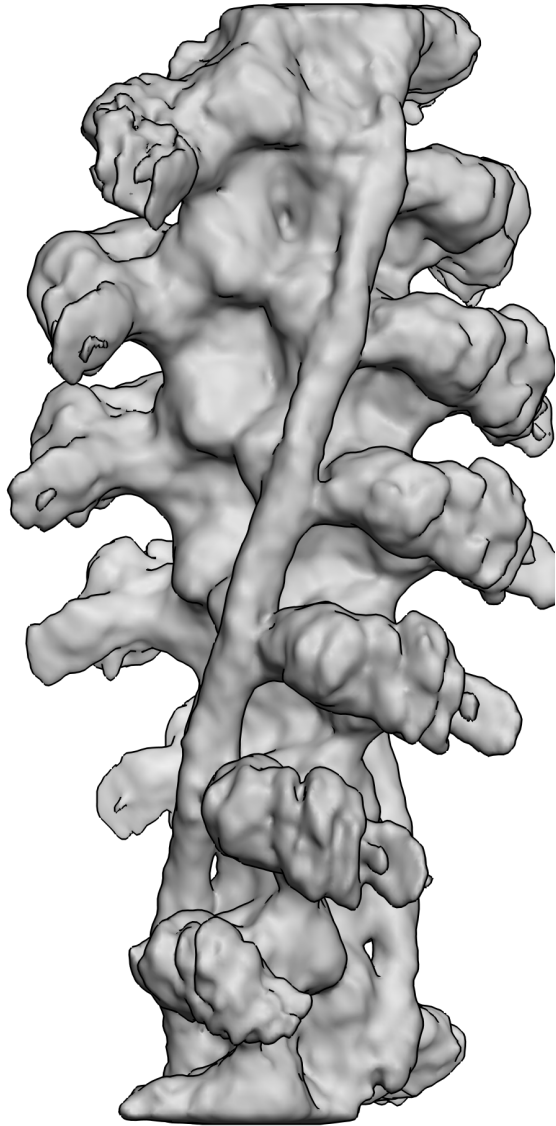


# Actin-Tropomyosin-Myosin Complex

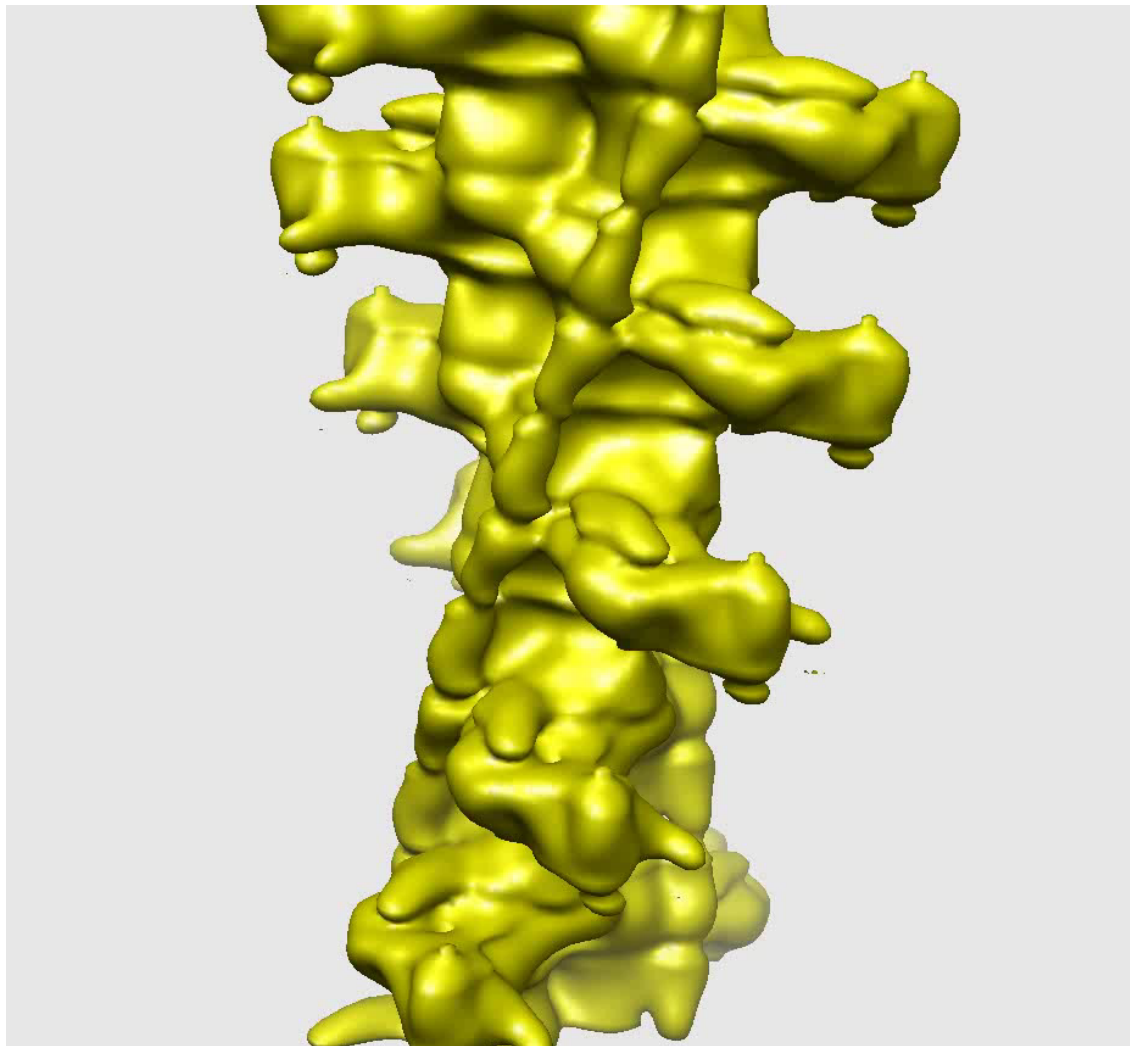
- JEOL 200 kV EM, 8k CCD  
Selected decorated filaments (B):  
Number of filaments: 7,696  
Number of segments: 35,319  
Pixel size 1.84 Å
- Helical symmetry parameters:  
rise  $\Delta z = 27.6 \text{ \AA}$   
azimuthal rotation  $166.5^\circ$



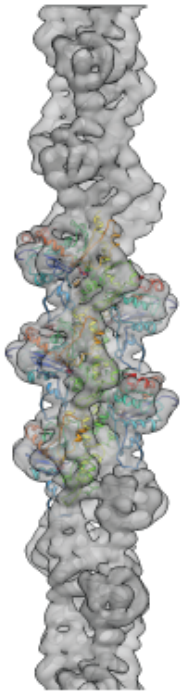
# Using the Asymmetric Unit for helical PCA



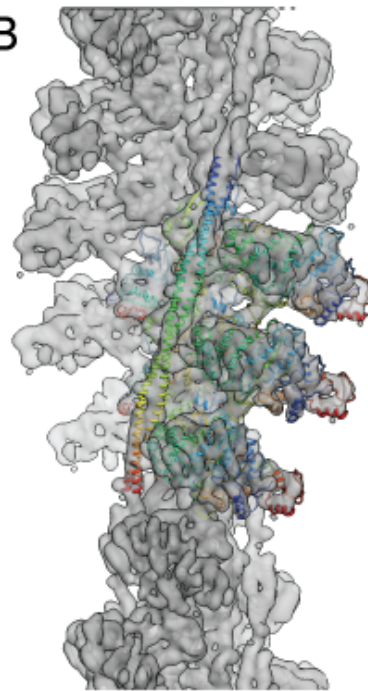
# Conformational modes of the Actin-Tropomyosin-Myosin complex



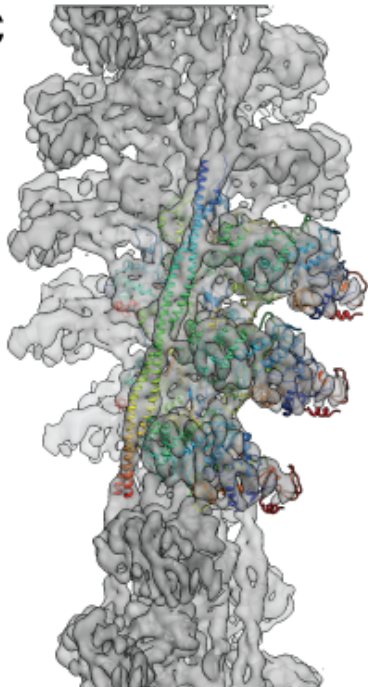
A



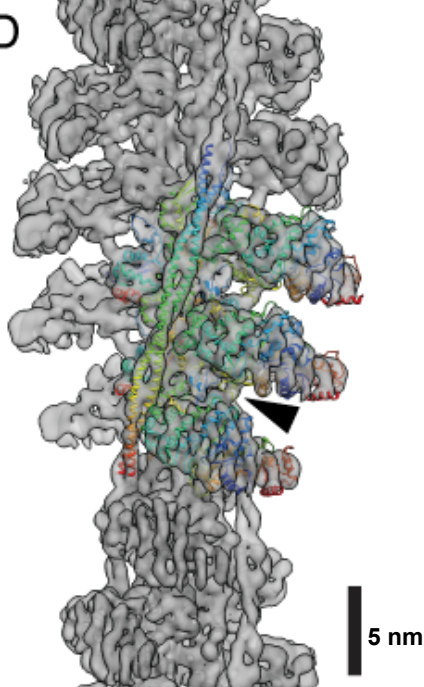
B



C



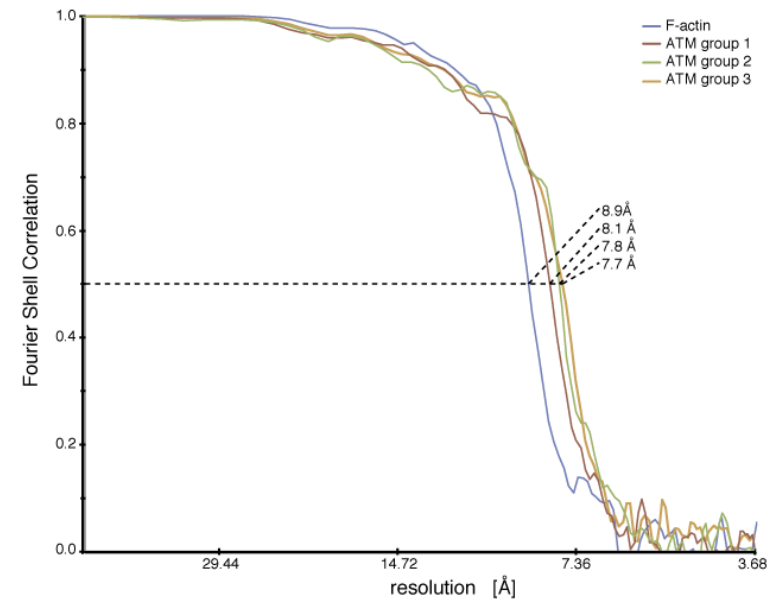
D



Structures of:

(A) undecorated F-actin filament

(B-D) three groups of decorated Actin-Tropomyosin-Myosin complex conformers (B-D)



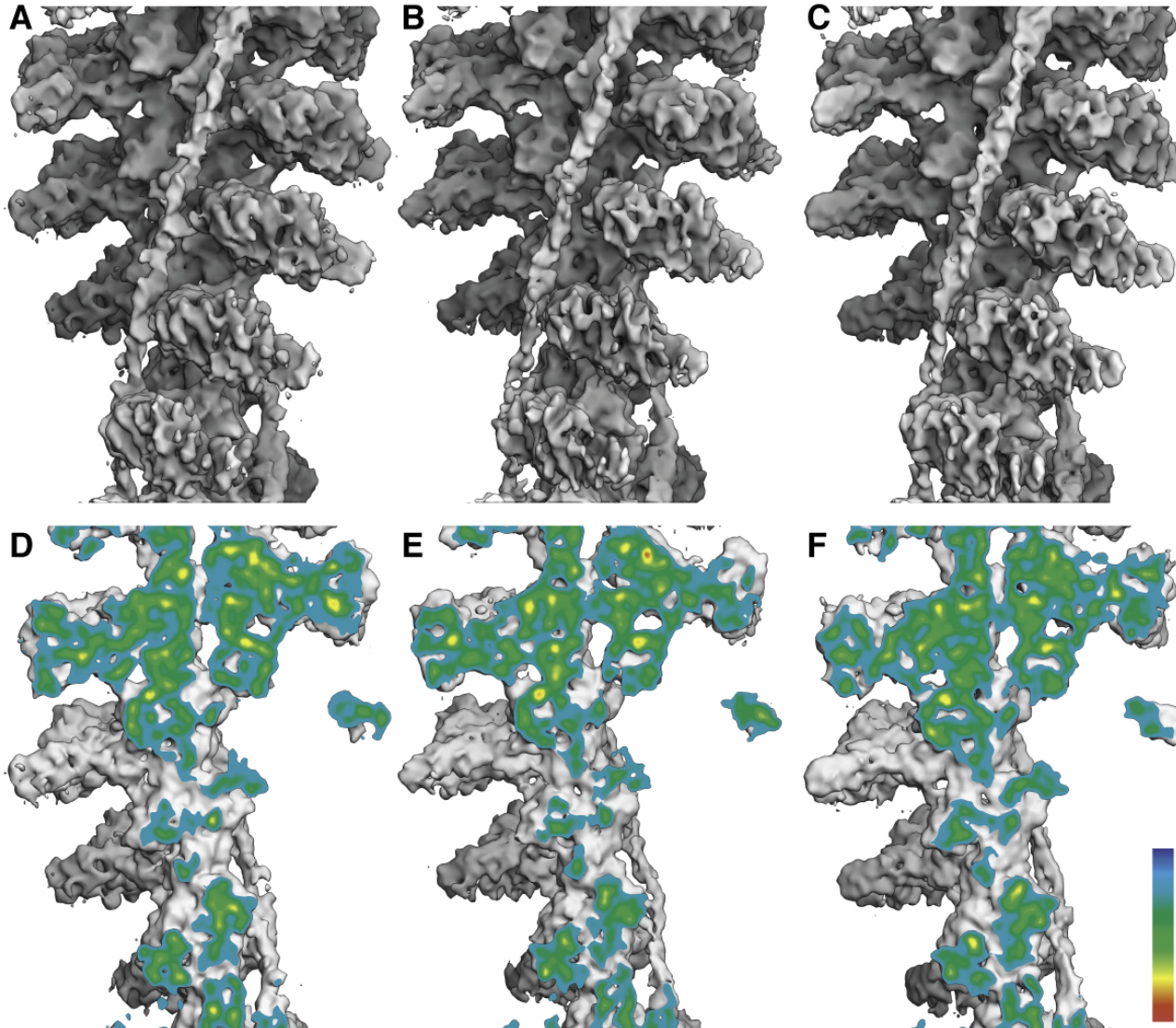
# Three states of the Actin-Tropomyosin-Myosin complex determined by hPCA (resolution 8Å)

20,686 segments

27%

47%

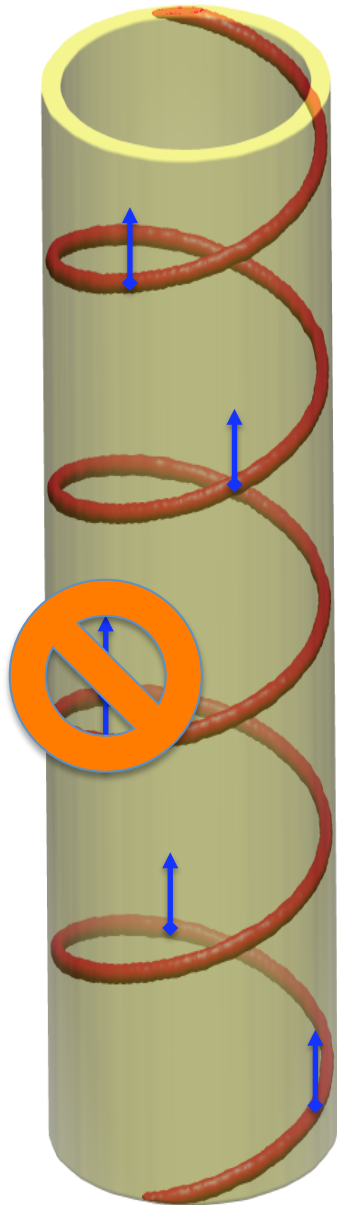
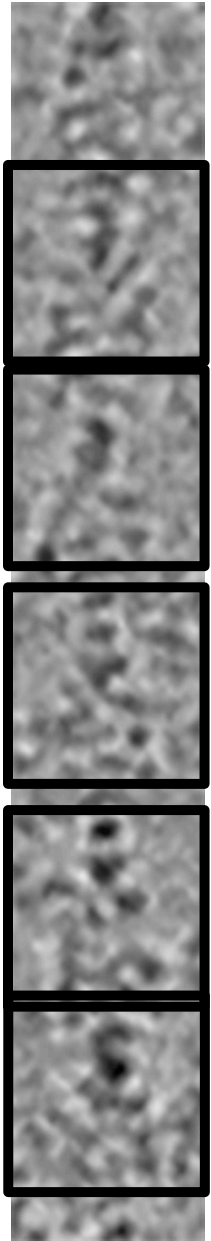
26%



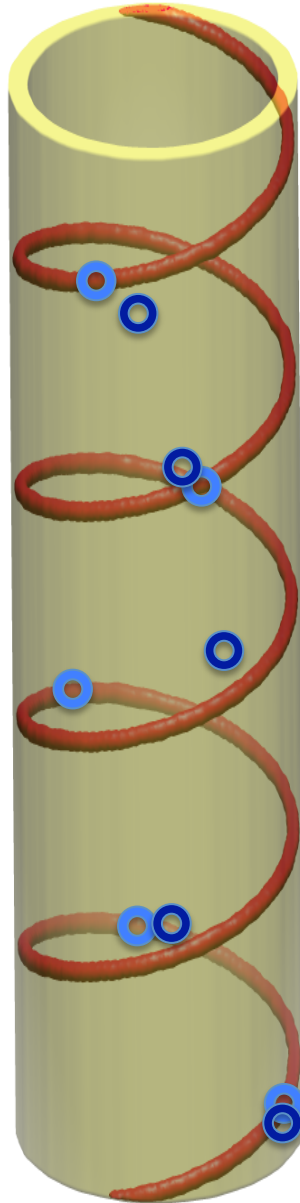
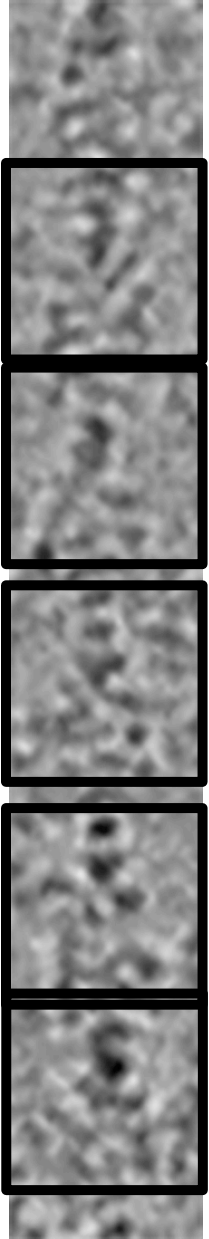


IHRSR segments are not independent

# Fundamental Geometrical Consistency up/down



# Geometrical Consistency helical



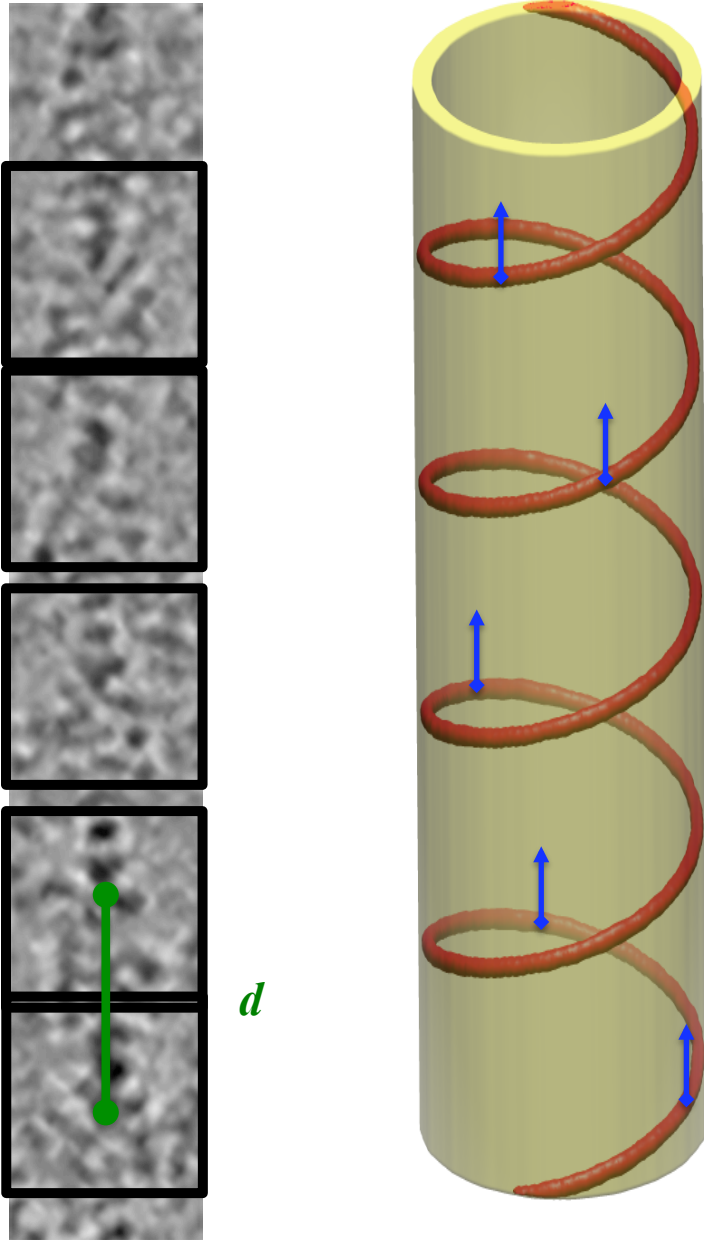
- ◆ Helical consistency would require a physical model of filament flexibility



# The Design of Geometrically Consistent IHRSR (gcIHRSR)

1. Prediction of orientation parameters based on assumed helical symmetry
2. Cooperative initial structure determination (only per-filament changes are allowed)
3. High-accuracy structure refinement (only restricted changes per segment are allowed)

# 1. Prediction of orientation parameters based on assumed helical symmetry

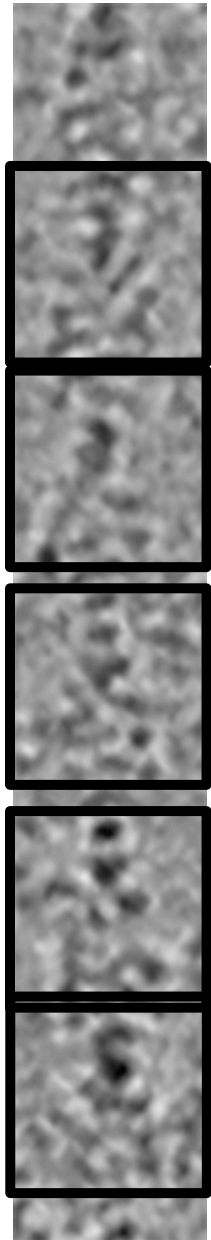


$$f(r, \varphi, z) = f(r, \varphi + n\Delta\varphi, z + n\Delta z), \quad n = \pm 1, \pm 2, \dots$$

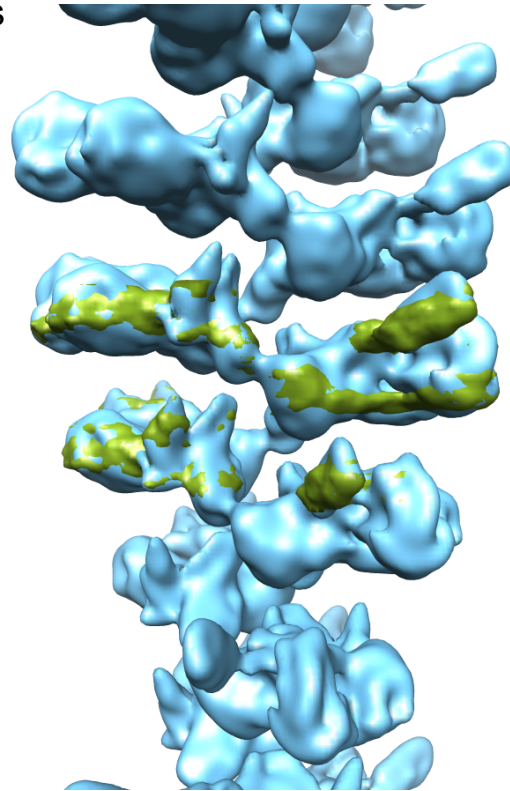
For each segment we have to assign  $\varphi$  and  $z$ :

1. first segment:  $\varphi=0$  and  $z=0$
2. second segment:  
given  $d$ ,  $\varphi = (d/\Delta z) \Delta\varphi$  and  $z = \text{mod}(d, \Delta z)$
3. and so on ....

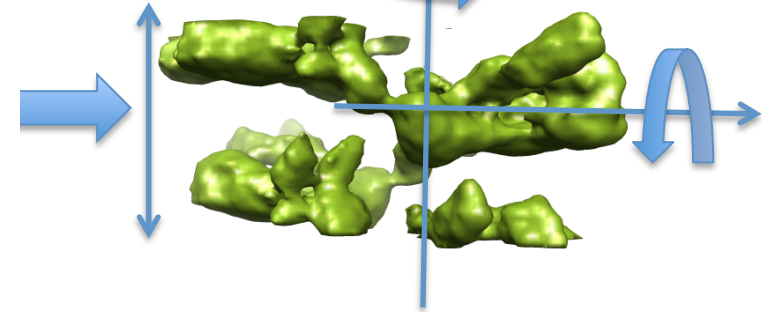
## 2. Cooperative initial structure determination, aka *Disk Alignment*



For each filament compute corresponding helical structure using predicted parameters



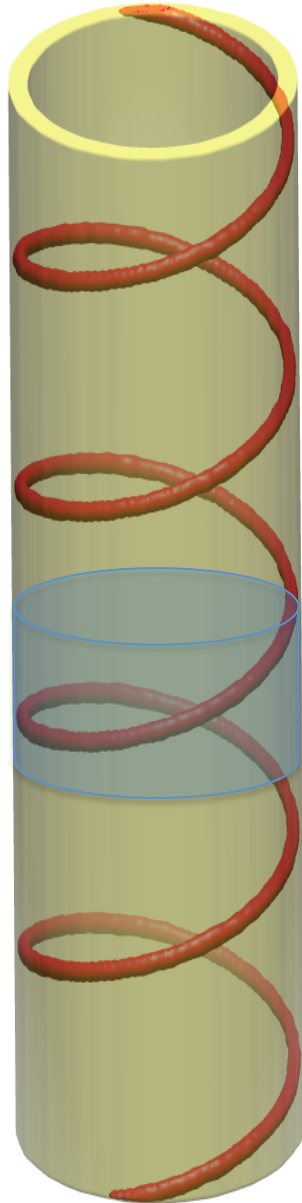
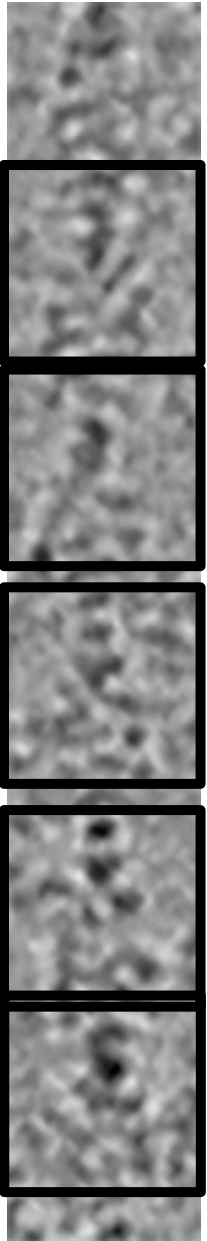
Extract a disk one rise high



Reference-free alignment of all filament disks determines rotation and translation of each filament/disk.

The resulting parameters are transferred to segments.

### 3. High-accuracy structure refinement (only restricted changes per segment allowed)



$$f(r, \varphi, z) = f(r, \varphi + n\Delta\varphi, z + n\Delta z), \quad n = \pm 1, \pm 2, \dots$$

Restriction of searches:

translation  $t_y$  no more than one rise:  $|t_y| < \Delta z / 2$

azimuthal angle  $\varphi \cong (t_y / \Delta z) \Delta\varphi$

*OUT OF PLANE TILT!*

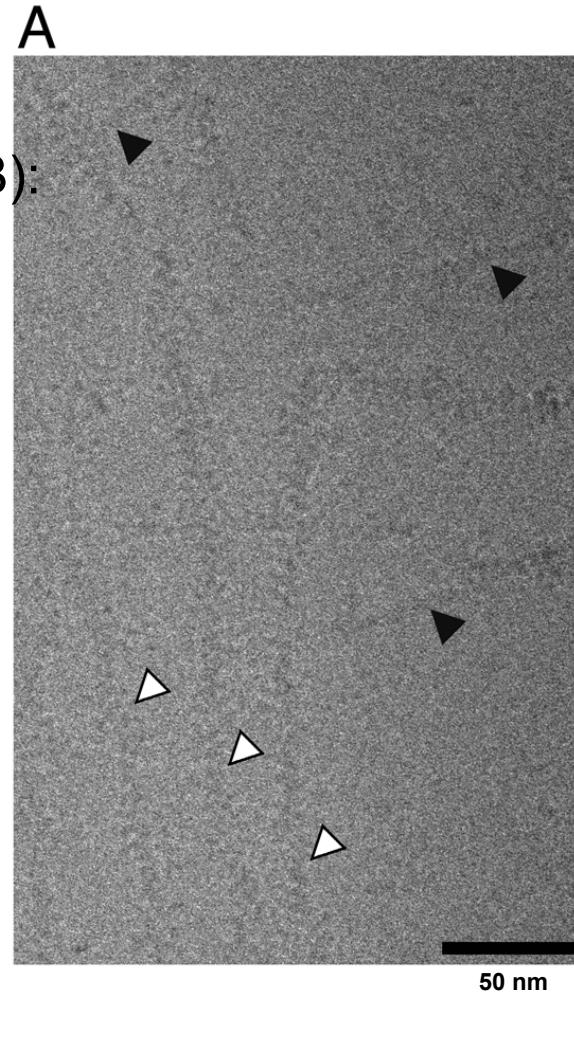
# Actin-Tropomyosin-Myosin Complex

segments per filament      segments      cumulative

51%

- JEOL 200 kV EM, 8k CCD  
Selected decorated filaments (B):  
Number of filaments: 7,696  
Number of segments: 35,319  
Pixel size 1.84 Å

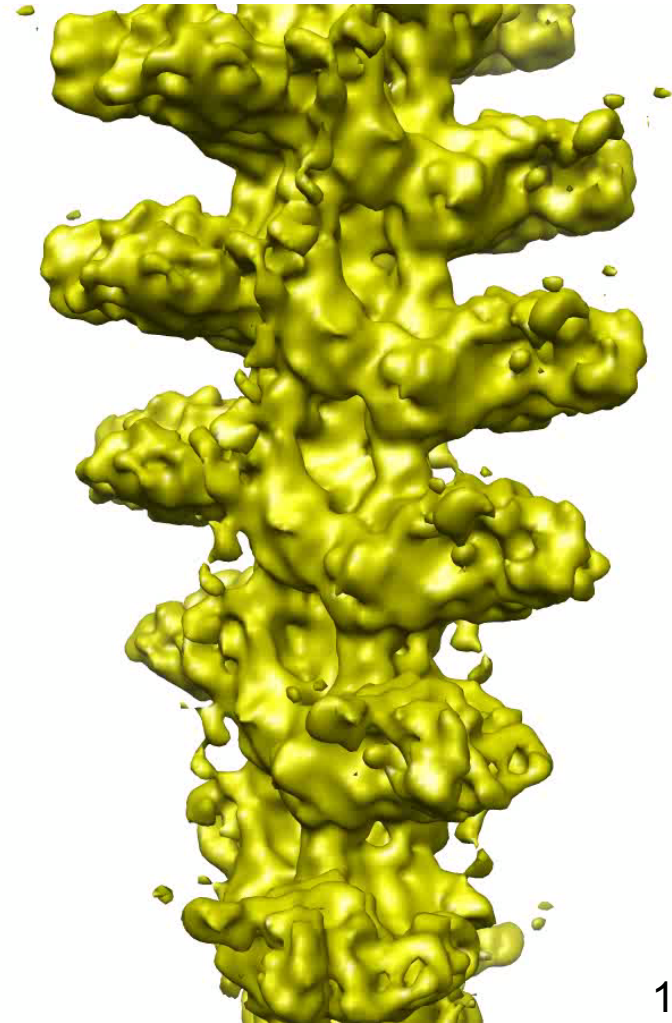
- Helical symmetry parameters:  
rise                     $\Delta z = 27.6 \text{ \AA}$   
                              (15 pixels)  
azimuthal rotation 166.5°



|    |      |       |
|----|------|-------|
| 7  | 2541 | 18055 |
| 8  | 2520 | 15514 |
| 9  | 1962 | 12994 |
| 10 | 2130 | 11032 |
| 11 | 1419 | 8902  |
| 12 | 984  | 7483  |
| 13 | 1066 | 6499  |
| 14 | 1050 | 5433  |
| 15 | 660  | 4383  |
| 16 | 592  | 3723  |
| 17 | 612  | 3131  |
| 18 | 288  | 2519  |
| 19 | 247  | 2231  |
| 20 | 240  | 1984  |
| 21 | 336  | 1744  |
| 22 | 242  | 1408  |
| 23 | 161  | 1166  |
| 24 | 120  | 1005  |
| 25 | 175  | 885   |
| 26 | 156  | 710   |
| 27 | 81   | 554   |
| 28 | 84   | 473   |
| 29 | 116  | 389   |
| 30 | 60   | 273   |
| 31 | 62   | 213   |
| 32 | 0    | 151   |
| 33 | 0    | 151   |
| 34 | 34   | 151   |
| 35 | 35   | 117   |
| 36 | 0    | 82    |
| 37 | 0    | 82    |
| 38 | 38   | 82    |
| 39 | 0    | 44    |
| 40 | 0    | 44    |
| 41 | 0    | 44    |
| 42 | 0    | 44    |
| 43 | 0    | 44    |
| 44 | 44   | 44    |

# ATM complex IHRSR versus GCihrrsr

Disk alignment  
number of filaments 1,705



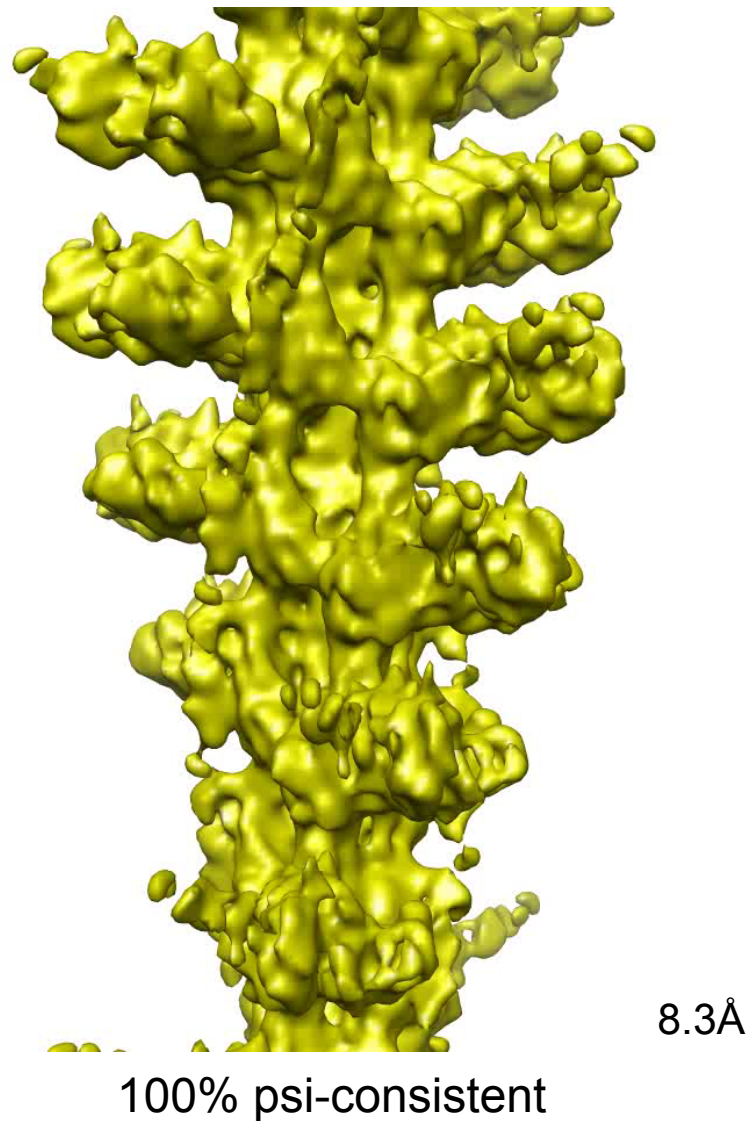
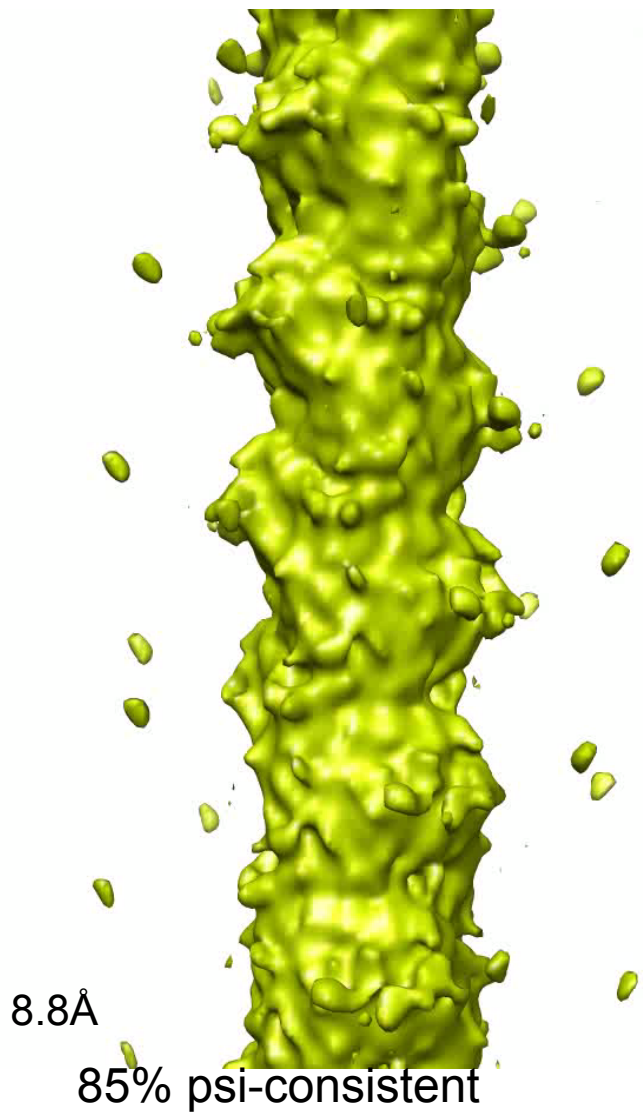
18.4Å

100% consistent

# ATM complex IHRSR versus GCihrsr

Exhaustive search

Constrained search

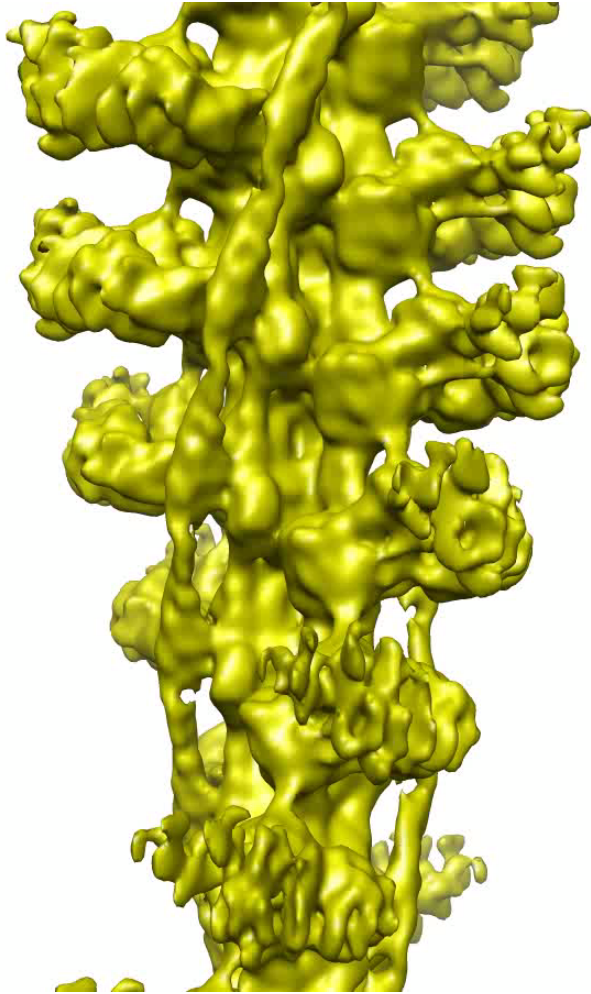


# ATM complex

## IHRSR versus GCihrsr

out-of-plane tilt:  $85 < \theta < 95$

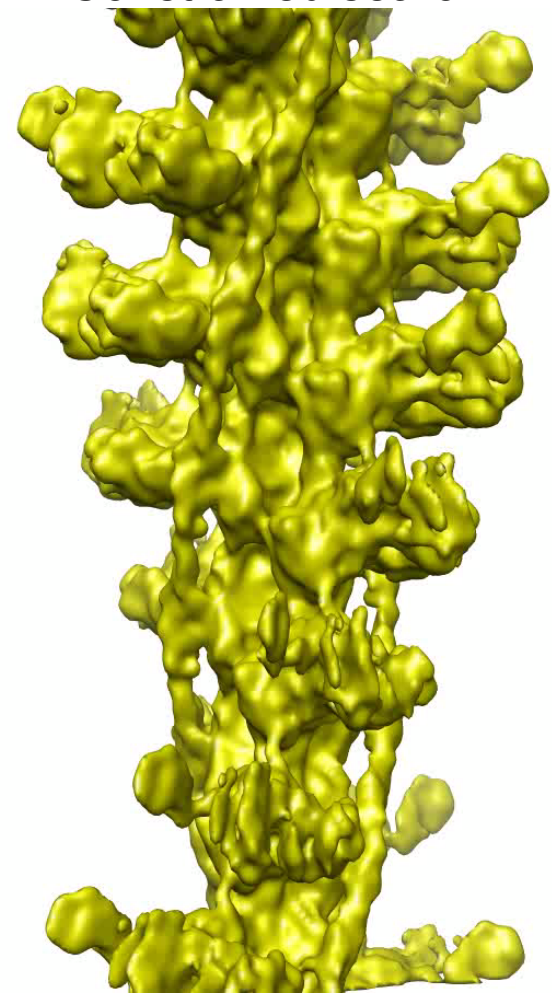
Exhaustive search



8.4Å

85% psi-consistent

Constrained search

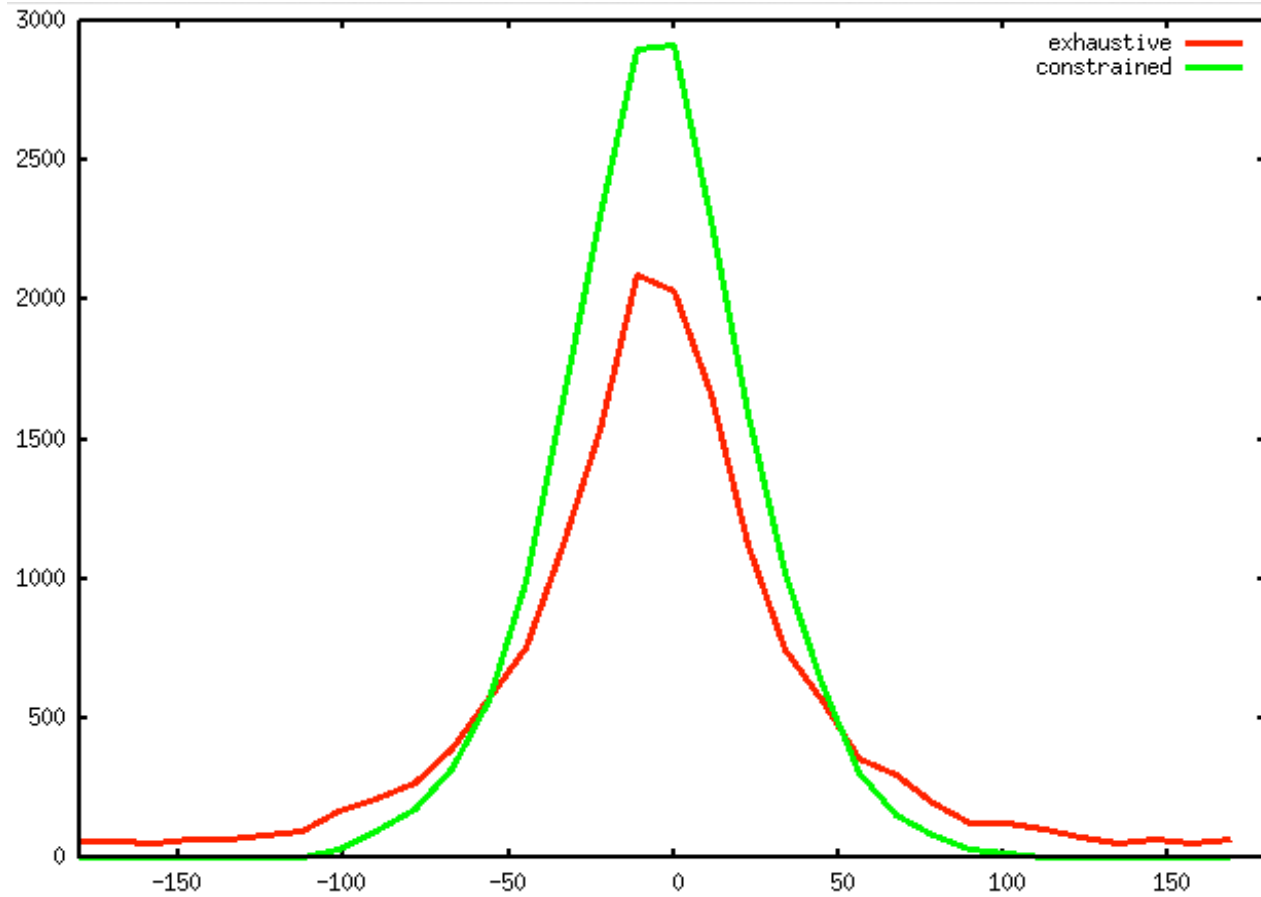


8.3Å

100% psi-consistent



# ATM complex IHRSR versus GCihrrsr



$$\Delta\varphi = 166.5^\circ$$

$$\Delta z = 15$$

azimuthal angle error  
difference between actual and predicted

# ATM complex IHRSR versus GCihrsr

$$\Delta\varphi = 166.5^\circ \quad \Delta z = 15$$

$\varphi$     $\theta$     $\psi$     $t_x$     $t_y$

| <b>Predicted</b> |    |    |   |             |
|------------------|----|----|---|-------------|
| 0                | 90 | 90 | 0 | 0           |
| 333              | 90 | 90 | 0 | -9.3681e-05 |
| 279              | 90 | 90 | 0 | 6.7365e-05  |
| 117              | 90 | 90 | 0 | 5.1956e-05  |
| 90               | 90 | 90 | 0 | -4.1725e-05 |
| 63               | 90 | 90 | 0 | 1.4733e-05  |
| 36               | 90 | 90 | 0 | -7.8948e-05 |
| 9                | 90 | 90 | 0 | -2.249e-05  |

| <b>Disk/<math>t_x</math> alignment</b> |    |       |       |     |
|--|----|-------|-------|-----|
| 329.9                                  | 90 | 270.0 | -18.0 | 6.0 |
| 356.9                                  | 90 | 270.0 | -15.0 | 6.0 |
| 50.9                                   | 90 | 270.0 | -18.0 | 6.0 |
| 212.9                                  | 90 | 270.0 | -15.0 | 6.0 |
| 239.9                                  | 90 | 270.0 | -15.0 | 6.0 |
| 266.9                                  | 90 | 270.0 | -15.0 | 6.0 |
| 293.9                                  | 90 | 270.0 | -15.0 | 6.0 |
| 320.9                                  | 90 | 270.0 | -15.0 | 6.0 |

| <b>Exhaustive</b> |    |       |       |      |
|-------------------|----|-------|-------|------|
| 47.0              | 90 | 87.2  | -4.0  | 0.0  |
| 91.0              | 90 | 276.7 | 3.0   | -2.8 |
| 122.0             | 90 | 277.4 | 8.0   | -3.8 |
| 217.0             | 90 | 271.8 | -5.7  | -2.0 |
| 308.0             | 90 | 277.4 | 2.0   | 1.9  |
| 291.0             | 90 | 88.9  | 5.4   | 4.8  |
| 305.0             | 90 | 90.0  | 1.0   | 0.0  |
| 1.0               | 90 | 85.7  | -13.0 | 1.9  |

| <b>Local</b> |    |       |       |     |
|--------------|----|-------|-------|-----|
| 326.0        | 90 | 277.4 | -13.0 | 3.6 |
| 359.0        | 90 | 263.3 | -12.0 | 5.4 |
| 94.0         | 90 | 263.3 | -19.0 | 2.4 |
| 223.0        | 90 | 273.2 | -23.0 | 6.4 |
| 250.0        | 90 | 271.1 | -24.0 | 7.5 |
| 273.0        | 90 | 265.4 | -20.0 | 9.6 |
| 305.0        | 90 | 272.8 | -23.0 | 9.2 |
| 311.0        | 90 | 267.9 | -21.0 | 9.2 |

# Conclusions/Future work

- ✓ Geometrically Consistent IHRSR is the correct approach to helical filament structure determination:
  - improved details
  - reduced fake resolution
  
- ? Cooperative local searches.
  
- ? Modeling of flexibility ?

# Acknowledgments

**Stefan Raunser**  
**MPI, Dortmund**



Max Planck Institute of  
Molecular Physiology

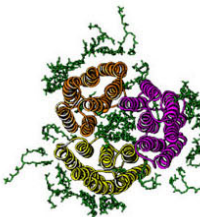
**Elmar Behrmann**  
**Charité, Berlin**



**Ed Egelman**  
**University of Virginia**



**David Stokes**  
**NYU Medical Center**



**NIH**